20. BIG-BANG NUCLEOSYNTHESIS

Revised August 2009 by B.D. Fields (Univ. of Illinois) and S. Sarkar (Univ. of Oxford).

Big-Bang nucleosynthesis (BBN) offers the deepest reliable probe of the early Universe, being based on well-understood Standard Model physics [1–5]. Predictions of the abundances of the light elements, D, ^{3}He, ^{4}He, and ^{7}Li, synthesized at the end of the 'first three minutes', are in good overall agreement with the primordial abundances inferred from observational data, thus validating the standard hot Big-Bang cosmology (see [6] for a review). This is particularly impressive given that these abundances span nine orders of magnitude – from $^4\mathrm{He/H} \sim 0.08$ down to $^7\mathrm{Li/H} \sim 10^{-10}$ (ratios by number). Thus BBN provides powerful constraints on possible deviations from the standard cosmology [2], and on new physics beyond the Standard Model [3,4].

20.1. Theory

The synthesis of the light elements is sensitive to physical conditions in the early radiation-dominated era at a temperature $T \sim 1$ MeV, corresponding to an age $t \sim 1$ s. At higher temperatures, weak interactions were in thermal equilibrium, thus fixing the ratio of the neutron and proton number densities to be $n/p = \mathrm{e}^{-Q/T}$, where $Q = 1.293$ MeV is the neutron-proton mass difference. As the temperature dropped, the neutron-proton inter-conversion rate, $\Gamma_{n \leftrightarrow p} \sim G_\mathrm{F}^2 T^5$, fell faster than the Hubble expansion rate, $H \sim \sqrt{g_* G_\mathrm{N}}\, T^2$, where g_* counts the number of relativistic particle species determining the energy density in radiation (see 'Big Bang Cosmology' review). This resulted in departure from chemical equilibrium ('freeze-out') at $T_\mathrm{fr} \sim (g_* G_\mathrm{N}/G_\mathrm{F}^4)^{1/6} \simeq 1$ MeV. The neutron fraction at this time, $n/p = \mathrm{e}^{-Q/T_\mathrm{fr}} \simeq 1/6$, is thus sensitive to every known physical interaction, since Q is determined by both strong and electromagnetic interactions while T_fr depends on the weak as well as gravitational interactions. Moreover, the sensitivity to the Hubble expansion rate affords a probe of *e.g.,* the number of relativistic neutrino species [7]. After freeze-out, the neutrons were free to β-decay, so the neutron fraction dropped to $n/p \simeq 1/7$ by the time nuclear reactions began. A simplified analytic model of freeze-out yields the n/p ratio to an accuracy of $\sim 1\%$ [8,9].

The rates of these reactions depend on the density of baryons (strictly speaking, nucleons), which is usually expressed normalized to the relic blackbody photon density as $\eta \equiv n_\mathrm{b}/n_\gamma$. As we shall see, all the light-element abundances can be explained with $\eta_{10} \equiv \eta \times 10^{10}$ in the range 5.1–6.5 (95% CL). With n_γ fixed by the present CMB temperature 2.725 K (see 'Cosmic Microwave Background' review), this can be stated as the allowed range for the baryon mass density today, $\rho_\mathrm{b} = (3.5\text{–}4.5) \times 10^{-31}\ \mathrm{g\,cm^{-3}}$, or as the baryonic fraction of the critical density, $\Omega_\mathrm{b} = \rho_\mathrm{b}/\rho_\mathrm{crit} \simeq \eta_{10} h^{-2}/274 = (0.019\text{–}0.024) h^{-2}$, where $h \equiv H_0/100\ \mathrm{km\,s^{-1}\,Mpc^{-1}} = 0.72 \pm 0.08$ is the present Hubble parameter (see Cosmological Parameters review).

The nucleosynthesis chain begins with the formation of deuterium in the process $p(n,\gamma)\mathrm{D}$. However, photo-dissociation by the high number density of photons delays production of deuterium (and other complex nuclei) well after T drops below the binding energy of deuterium, $\Delta_\mathrm{D} = 2.23$ MeV. The quantity $\eta^{-1}\mathrm{e}^{-\Delta_\mathrm{D}/T}$, *i.e.,* the number of

photons per baryon above the deuterium photo-dissociation threshold, falls below unity at $T \simeq 0.1$ MeV; nuclei can then begin to form without being immediately photo-dissociated again. Only 2-body reactions, such as $\mathrm{D}(p,\gamma)^3\mathrm{He}$, $^3\mathrm{He}(\mathrm{D},p)^4\mathrm{He}$, are important because the density by this time has become rather low – comparable to that of air!

Nearly all the surviving neutrons when nucleosynthesis begins end up bound in the most stable light element ^{4}He. Heavier nuclei do not form in any significant quantity both because of the absence of stable nuclei with mass number 5 or 8 (which impedes nucleosynthesis via n^4He, p^4He or ^{4}He^{4}He reactions), and the large Coulomb barriers for reactions such as $\mathrm{T}(^4\mathrm{He},\gamma)^7\mathrm{Li}$ and $^3\mathrm{He}(^4\mathrm{He},\gamma)^7\mathrm{Be}$. Hence the primordial mass fraction of ^{4}He, conventionally referred to as Y_p, can be estimated by the simple counting argument

$$Y_\mathrm{p} = \frac{2(n/p)}{1+n/p} \simeq 0.25 \ . \tag{20.1}$$

There is little sensitivity here to the actual nuclear reaction rates, which are, however, important in determining the other 'left-over' abundances: D and ^{3}He at the level of a few times 10^{-5} by number relative to H, and ^{7}Li/H at the level of about 10^{-10} (when η_{10} is in the range 1–10). These values can be understood in terms of approximate analytic arguments [9,10]. The experimental parameter most important in determining Y_p is the neutron lifetime, τ_n, which normalizes (the inverse of) $\Gamma_{n\to p}$. The experimental uncertainty in τ_n used to be a source of concern, but has been reduced substantially: $\tau_n = 885.7 \pm 0.8$ s (see N Baryons Listing).

The elemental abundances shown in Fig. 20.1 as a function of η_{10} were calculated [11] using an updated version [12] of the Wagoner code [1]; other modern versions [13,14] are publicly available. The ^{4}He curve includes small corrections due to radiative processes at zero and finite temperatures [15], non-equilibrium neutrino heating during $e^\pm$ annihilation [16], and finite nucleon mass effects [17]; the range reflects primarily the 2σ uncertainty in the neutron lifetime. The spread in the curves for D, ^{3}He, and ^{7}Li corresponds to the 2σ uncertainties in nuclear cross sections, as estimated by Monte Carlo methods [18–19]. The input nuclear data have been carefully reassessed [11, 20-23], leading to improved precision in the abundance predictions. In particular, the uncertainty in ^{7}Li/H at interesting values of η has been reduced recently by a factor ~ 2, a consequence of a similar reduction in the error budget [24] for the dominant mass-7 production channel $T(^4\mathrm{He},\gamma)^7\mathrm{Be}$. Polynomial fits to the predicted abundances and the error correlation matrix have been given [19,25]. The boxes in Fig. 20.1 show the observationally inferred primordial abundances with their associated statistical and systematic uncertainties, as discussed below.

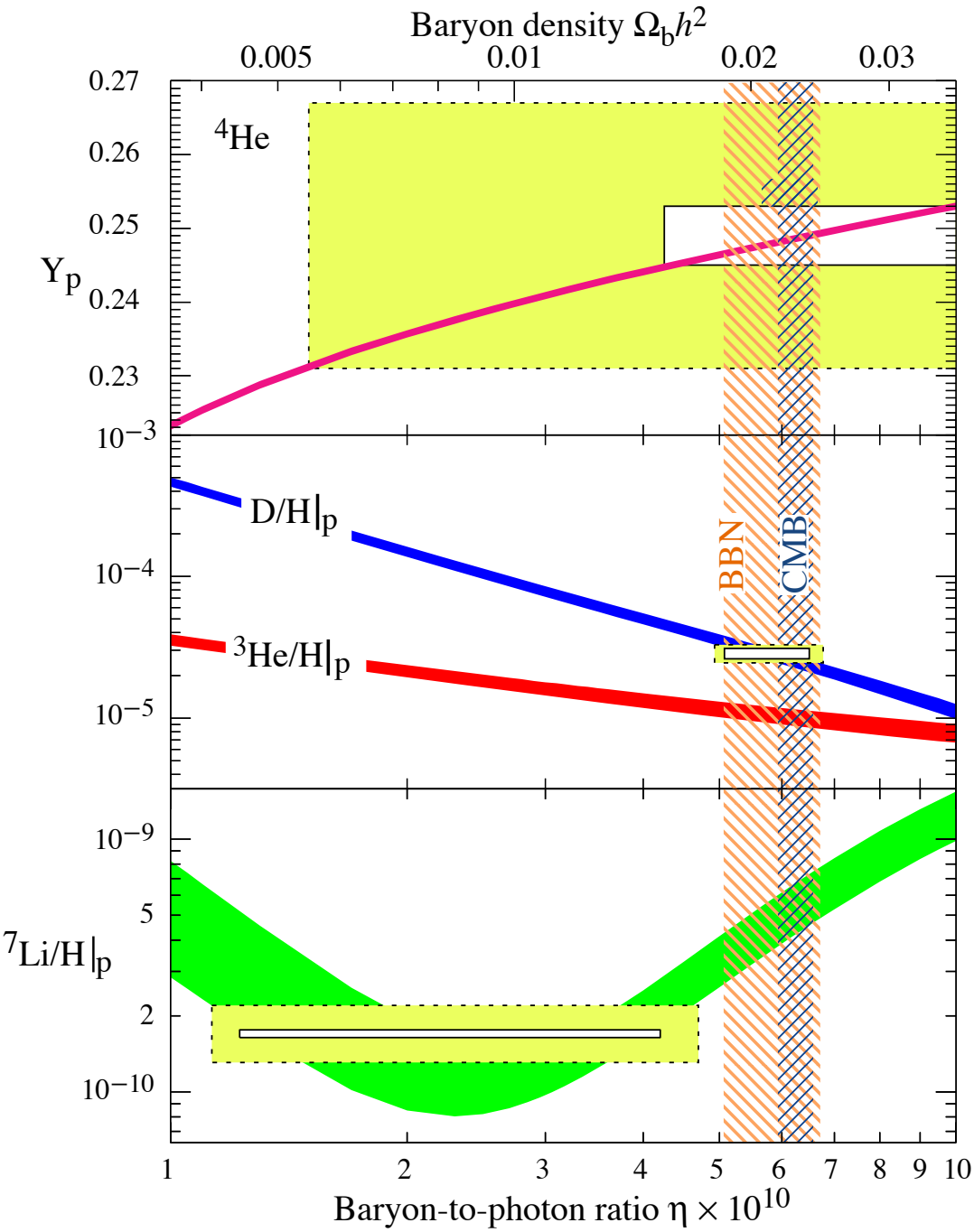

Figure 20.1: The abundances of ^{4}He, D, ^{3}He, and ^{7}Li as predicted by the standard model of Big-Bang nucleosynthesis [11] – the bands show the 95% CL range. Boxes indicate the observed light element abundances (smaller boxes: $\pm 2\sigma$ statistical errors; larger boxes: $\pm 2\sigma$ statistical *and* systematic errors). The narrow vertical band indicates the CMB measure of the cosmic baryon density, while the wider band indicates the BBN concordance range (both at 95% CL). Color version at end of book.

20.2. Light Element Abundances

BBN theory predicts the universal abundances of D, ^{3}He, ^{4}He, and ^{7}Li, which are essentially fixed by $t \sim 180$ s. Abundances are, however, observed at much later epochs, after stellar nucleosynthesis has commenced. The ejected remains of this stellar processing can alter the light element abundances from their primordial values, and also produce heavy elements such as C, N, O, and Fe ('metals'). Thus, one seeks astrophysical sites with low metal abundances, in order to measure light element abundances which are closer to primordial. For all of the light elements, systematic errors are an important (and often dominant) limitation to the precision with which primordial abundances can be inferred.

High-resolution spectra reveal the presence of D in high-redshift, low-metallicity quasar absorption systems via its isotope-shifted Lyman-α absorption [26–29]. It is believed that there are no astrophysical sources of deuterium [30], so any detection provides a lower limit to primordial D/H, and thus an upper limit on η; for example, the local interstellar value of $\mathrm{D/H}|_\mathrm{p} = (1.56 \pm 0.04) \times 10^{-5}$ [31] requires $\eta_{10} \leq 9$. Recent observations find an unexpected scatter of a factor of ~ 2 [32], as well as correlations with heavy element abundances which suggest that interstellar D may suffer stellar processing (astration), but also partly reside in dust particles which evade gas-phase observations. This is supported by a measurement in the lower halo [33], which indicates that the Galactic D abundance has been reduced by a factor of only 1.12 ± 0.13 since its formation. For the high-redshift systems, conventional models of galactic nucleosynthesis (chemical evolution) do not predict either of these effects for D/H [34].

The observed extragalactic D values are bracketed by the non-detection of D in a high-redshift system, $\mathrm{D/H}|_\mathrm{p} < 6.7 \times 10^{-5}$ at 1σ [35], and low values in some (damped Lyman-α) systems [26,27]. Averaging the seven most precise observations of deuterium in quasar absorption systems gives $\mathrm{D/H} = (2.82 \pm 0.12) \times 10^{-5}$, where the error is statistical only [28,29]. However, there remains concern over systematic errors, the dispersion between the values being much larger than is expected from the individual measurement errors ($\chi^2 = 17.7$ for $\nu = 6$ d.o.f.). Increasing the error by a factor $\sqrt{\chi^2/\nu}$ gives, as shown in Fig. 20.1:

$$\mathrm{D/H}|_\mathrm{p} = (2.82 \pm 0.21) \times 10^{-5}. \tag{20.2}$$

^{4}He can be observed in clouds of ionized hydrogen (H II regions), the most metal-poor of which are in dwarf galaxies. There is now a large body of data on ^{4}He and CNO in such systems [36]. These data confirm that the small stellar contribution to helium is positively correlated with metal production. Extrapolating to zero metallicity gives the primordial ^{4}He abundance [37]

$$Y_\mathrm{p} = 0.249 \pm 0.009. \tag{20.3}$$

Here the latter error is a careful (and significantly enlarged) estimate of the systematic uncertainties which dominate, and is based on the scatter in different analyses of the physical properties of the H II regions [36,37]. Other recent extrapolations to zero

metallicity give $Y_{\rm p} = 0.247 \pm 0.001$ or 0.252 ± 0.001 depending on which set of He I emissivities are used [38], and $Y_{\rm p} = 0.248 \pm 0.003$ [39]. These are consistent (given the systematic errors) with the above estimate [37], which appears in Fig. 20.1.

As we will see in more detail below, the primordial abundance of lithium now plays a central role in BBN, and possibly points to new physics. The systems best suited for Li observations are metal-poor stars in the spheroid (Pop II) of our Galaxy, which have metallicities going down to at least 10^{-4}, and perhaps 10^{-5} of the Solar value [40]. Observations have long shown [41–45] that Li does not vary significantly in Pop IIstars with metallicities $\lesssim 1/30$ of Solar — the 'Spite plateau' [41]. Precision data suggest a small but significant correlation between Li and Fe [42], which can be understood as the result of Li production from Galactic cosmic rays [43]. Extrapolating to zero metallicity, one arrives at a primordial value $\mathrm{Li/H}|_{\rm p} = (1.23 \pm 0.06^{+0.68}_{-0.32}) \times 10^{-10}$ [44], where the first error given is statistical and is very small due to the relatively large sample of 22 stars used. One source of systematic error stems from the differences in techniques used to determine the physical parameters (*e.g.*, the temperature) of the stellar atmosphere in which the Li absorption line is formed. Alternative analyses, using methods that give systematically higher temperatures, and in some cases different stars and stellar systems (globular clusters), yield $\mathrm{Li/H}|_{\rm p} = (2.19 \pm 0.28) \times 10^{-10}$ [45], $\mathrm{Li/H}|_{\rm p} = (2.34 \pm 0.32) \times 10^{-10}$ [46], and $\mathrm{Li/H}|_{\rm p} = (1.26 \pm 0.26) \times 10^{-10}$ [47]; the differences with [44] indicate a systematic uncertainty of a factor of ~ 2. Moreover, it is possible that the Li in Pop II stars has been partially destroyed, due to mixing of the outer layers with the hotter interior [48]. Such processes can be constrained by the absence of significant scatter in Li versus Fe [42], and by observations of the fragile isotope ^{6}Li [43]. Nevertheless, some depletion is likely to exist, though this is difficult to quantify with confidence – a factor as large as ~ 1.8 has been suggested [49]. Including these systematics, we estimate a primordial Li range which spans the ranges above, as shown in Fig. 20.1:

$$\mathrm{Li/H}|_{\rm p} = (1.7 \pm 0.06 \pm 0.44) \times 10^{-10}. \tag{20.4}$$

Stellar determination of Li abundances typically sum over both stable isotopes ^{6}Li and ^{7}Li. Recent high-precision measurements are sensitive to the tiny isotopic shift in Li absorption (which manifests itself in the shape of the blended, thermally broadened line) and indicate $^6\mathrm{Li}/^7\mathrm{Li} \leq 0.15$ [50]. This confirms that ^{7}Li is dominant, but surprisingly there is indication of a ^{6}Li plateau (analogous to the ^{7}Li plateau) which suggests a significant primordial ^{6}Li abundance. However, caution must be exercised since convective motions in the star can generate similar asymmetries in the line shape, hence the deduced ^{6}Li abundance is presently best interpreted as an upper limit [51].

Turning to ^{3}He, the only data available are from the Solar system and (high-metallicity) H II regions in our Galaxy [52]. This makes inferring the primordial abundance difficult, a problem compounded by the fact that stellar nucleosynthesis models for ^{3}He are in conflict with observations [53]. Consequently, it is no longer appropriate to use ^{3}He as a cosmological probe; instead, one might hope to turn the problem around and constrain stellar astrophysics using the predicted primordial ^{3}He abundance [54].

20.3. Concordance, Dark Matter, and the CMB

We now use the observed light element abundances to test the theory. We first consider standard BBN, which is based on Standard Model physics alone, so $N_\nu = 3$ and the only free parameter is the baryon-to-photon ratio η. (The implications of BBN for physics beyond the Standard Model will be considered below, §4). Thus, any abundance measurement determines η, while additional measurements overconstrain the theory and thereby provide a consistency check.

First we note that the overlap in the η ranges spanned by the larger boxes in Fig. 20.1 indicates overall concordance. More quantitatively, when we account for theoretical uncertainties, as well as the statistical and systematic errors in observations, there is acceptable agreement among the abundances when

$$5.1 \leq \eta_{10} \leq 6.5 \text{ (95\% CL)}. \tag{20.5}$$

However, the agreement is much less satisfactory if we use only the quoted statistical errors in the observations. In particular, as seen in Fig. 20.1, D and ^{4}He are consistent with each other, but favor a value of η which is higher by a factor of at least 2.4, and by at least $\sim 4.2\sigma$ from that indicated by the ^{7}Li abundance determined in stars. Furthermore, if the ^{6}Li plateau [50] reflects a primordial component, it is ~ 1000 times that expected in standard BBN; both these "lithium problems" may indicate new physics (see below).

Even so, the overall concordance is remarkable: using well-established microphysics we have extrapolated back to an age of ~ 1 s to correctly predict light element abundances spanning 9 orders of magnitude. This is a major success for the standard cosmology, and inspires confidence in extrapolation back to still earlier times.

This concordance provides a measure of the baryon content

$$0.019 \leq \Omega_{\rm b} h^2 \leq 0.024 \text{ (95\% CL)}, \tag{20.6}$$

a result that plays a key role in our understanding of the matter budget of the Universe. First we note that $\Omega_{\rm b} \ll 1$, *i.e.*, baryons cannot close the Universe [55]. Furthermore, the cosmic density of (optically) luminous matter is $\Omega_{\rm lum} \simeq 0.0024 h^{-1}$ [56], so that $\Omega_{\rm b} \gg \Omega_{\rm lum}$: most baryons are optically dark, probably in the form of a diffuse intergalactic medium [57]. Finally, given that $\Omega_{\rm m} \sim 0.3$ (see Dark Matter and Cosmological Parameters reviews), we infer that most matter in the Universe is not only dark, but also takes some non-baryonic (more precisely, non-nucleonic) form.

The BBN prediction for the cosmic baryon density can be tested through precision observations of CMB temperature fluctuations (see Cosmic Microwave Background review). One can determine η from the amplitudes of the acoustic peaks in the CMB angular power spectrum [58], making it possible to compare two measures of η using very different physics, at two widely separated epochs. In the standard cosmology, there is no change in η between BBN and CMB decoupling, thus, a comparison of $\eta_{\rm BBN}$ and $\eta_{\rm CMB}$ is a key test. Agreement would endorse the standard picture while disagreement could point to new physics during/between the BBN and CMB epochs.

The release of the WMAP results was a landmark event in this test of BBN. As with other cosmological parameter determinations from CMB data, the derived $\eta_{\rm CMB}$ depends on the adopted priors [59], in particular the form assumed for the power spectrum of primordial density fluctuations. If this is taken to be a scale-free power-law, the five-year WMAP data imply $\Omega_{\rm b}h^2 = 0.02273 \pm 0.00062$ or $\eta_{10} = 6.23 \pm 0.17$ [60] as shown in Fig. 20.1. Other assumptions for the shape of the power spectrum can lead to baryon densities as low as $\Omega_{\rm b}h^2 = 0.0175 \pm 0.0007$ [61]. Thus, outstanding uncertainties regarding priors are a source of systematic error which presently exceeds the statistical error in the prediction for η.

It is remarkable that the CMB estimate of the baryon density is consistent with the BBN range quoted in Eq. (20.6), and in very good agreement with the value inferred from recent high-redshift D/H measurements [29] and ^{4}He determinations; together these observations span diverse environments from redshifts $z = 1000$ to the present.

Bearing in mind the importance of priors, the promise of precision determinations of the baryon density using the CMB motivates the use of this value as an input to BBN calculations. Within the context of the Standard Model, BBN then becomes a zero-parameter theory, and the light element abundances are completely determined to within the uncertainties in $\eta_{\rm CMB}$ and the BBN theoretical errors. Comparison with the observed abundances then can be used to test the astrophysics of post-BBN light element evolution [64]. Alternatively, one can consider possible physics beyond the Standard Model (*e.g.*, which might change the expansion rate during BBN) and then use all of the abundances to test such models; this is the subject of our final section.

20.4. The Lithium Problem

As Fig. 20.1 shows, stellar Li/H measurements are inconsistent with the CMB (and D/H), given the error budgets we have quoted. Recent updates in nuclear cross sections, stellar abundance systematics, and the WMAP results all *increase* the discrepancy to as much as 5.3σ, depending on the stellar abundance analysis adopted. [11].

The question then becomes more pressing as to whether this mismatch comes from systematic errors in the observed abundances, and/or uncertainties in stellar astrophysics, or whether there might be new physics at work. Nucleosynthesis models in which the baryon-to-photon ratio is inhomogeneous can alter abundances for a given $\eta_{\rm BBN}$, but will overproduce ^{7}Li [62]. Entropy generation by some non-standard process could have decreased η between the BBN era and CMB decoupling, however the lack of spectral distortions in the CMB rules out any significant energy injection upto a redshift $z \sim 10^7$ [63]. The most intriguing resolution of the lithium problem thus involves new physics during BBN [4].

For now this is a central unresolved issue in BBN. Nevertheless, the remarkable concordance between the CMB and D/H, as well as ^{4}He, remain as non-trivial successes, and open windows onto the early Universe and particle physics, as we now discuss.

20.5. Beyond the Standard Model

Given the simple physics underlying BBN, it is remarkable that it still provides the most effective test for the cosmological viability of ideas concerning physics beyond the Standard Model. Although baryogenesis and inflation must have occurred at higher temperatures in the early Universe, we do not as yet have 'standard models' for these, so BBN still marks the boundary between the established and the speculative in Big Bang cosmology. It might appear possible to push the boundary back to the quark-hadron transition at $T \sim \Lambda_{\rm QCD}$, or electroweak symmetry breaking at $T \sim 1/\sqrt{G_{\rm F}}$; however, so far no observable relics of these epochs have been identified, either theoretically or observationally. Thus, although the Standard Model provides a precise description of physics up to the Fermi scale, cosmology cannot be traced in detail before the BBN era.

Limits on particle physics beyond the Standard Model come mainly from the observational bounds on the ^{4}He abundance. This is proportional to the n/p ratio which is determined when the weak-interaction rates fall behind the Hubble expansion rate at $T_{\rm fr} \sim 1$ MeV. The presence of additional neutrino flavors (or of any other relativistic species) at this time increases g_*, hence the expansion rate, leading to a larger value of $T_{\rm fr}$, n/p, and therefore $Y_{\rm p}$ [7,65]. In the Standard Model, the number of relativistic particle species at 1 MeV is $g_* = 5.5 + \frac{7}{4}N_\nu$, where the factor 5.5 accounts for photons and $e^\pm$, and N_ν is the *effective* number of (nearly massless) neutrino flavors (see Big Bang Cosmology review). The helium curves in Fig. 20.1 were computed taking $N_\nu = 3$; small corrections for non-equilibrium neutrino heating [16] are included in the thermal evolution and lead to an effective $N_\nu = 3.04$ compared to assuming instantaneous neutrino freezeout (see, *e.g.*, Big Bang Cosmology review). The computed ^{4}He abundance scales as $\Delta Y_{\rm p} \simeq 0.013 \Delta N_\nu$ [8]. Clearly the central value for N_ν from BBN will depend on η, which is independently determined (with weaker sensitivity to N_ν) by the adopted D or ^{7}Li abundance. For example, if the best value for the observed primordial ^{4}He abundance is 0.249, then, for $\eta_{10} \sim 6$, the central value for N_ν is very close to 3. This limit depends sensitively on the adopted light element abundances, particularly $Y_{\rm p}$. A maximum likelihood analysis on η and N_ν based on the above ^{4}He and D abundances finds the (correlated) 95% CL ranges to be $4.9 < \eta_{10} < 7.1$ and $1.8 < N_\nu < 4.5$ [66]. Similar results were obtained in another study [67] which presented a simpler method to extract such bounds based on χ^2 statistics, given a set of input abundances. Using the CMB determination of η improves the constraints: with a 'low' ^{4}He, $N_\nu = 3$ is barely allowed at 2σ [68], but using the ^{4}He (and D) abundance quoted above gives $5.66 < \eta_{10} < 6.58$ ($\Omega_{\rm b}h^2 = 0.0226 \pm 0.0017$) and $N_\nu = 3.2 \pm 1.2$ (95% CL) [66].

Just as one can use the measured helium abundance to place limits on g_* [65], any changes in the strong, weak, electromagnetic, or gravitational coupling constants, arising *e.g.*, from the dynamics of new dimensions, can be similarly constrained [69], as can be any speed-up of the expansion rate in *e.g.* scalar-tensor theories of gravity [70].

The limits on N_ν can be translated into limits on other types of particles or particle masses that would affect the expansion rate of the Universe during nucleosynthesis. For example, consider 'sterile' neutrinos with only right-handed interactions of strength $G_{\rm R} < G_{\rm F}$. Such particles would decouple at higher temperature than (left-handed)

neutrinos, so their number density ($\propto\ T^3$) relative to neutrinos would be reduced by any subsequent entropy release, *e.g.*, due to annihilations of massive particles that become non-relativistic between the two decoupling temperatures. Thus (relativistic) particles with less than full strength weak interactions contribute less to the energy density than particles that remain in equilibrium up to the time of nucleosynthesis [71]. If we impose $N_\nu < 4$ as an illustrative constraint, then the three right-handed neutrinos must have a temperature $3(T_{\nu_{\rm R}}/T_{\nu_{\rm L}})^4 < 1$. Since the temperature of the decoupled $\nu_{\rm R}$'s is determined by entropy conservation (see Big Bang Cosmology review), $T_{\nu_{\rm R}}/T_{\nu_{\rm L}} = [(43/4)/g_*(T_{\rm d})]^{1/3} < 0.76$, where $T_{\rm d}$ is the decoupling temperature of the $\nu_{\rm R}$'s. This requires $g_*(T_{\rm d}) > 24$, so decoupling must have occurred at $T_{\rm d} > 140$ MeV. The decoupling temperature is related to $G_{\rm R}$ through $(G_{\rm R}/G_{\rm F})^2 \sim (T_{\rm d}/3\,{\rm MeV})^{-3}$, where 3 MeV is the decoupling temperature for $\nu_{\rm L}$s. This yields a limit $G_{\rm R} \lesssim 10^{-2} G_{\rm F}$. The above argument sets lower limits on the masses of new Z' gauge bosons to which right-handed neutrinos would be coupled in models of superstrings [72], or extended technicolor [73]. Similarly a Dirac magnetic moment for neutrinos, which would allow the right-handed states to be produced through scattering and thus increase g_*, can be significantly constrained [74], as can any new interactions for neutrinos which have a similar effect [75]. Right-handed states can be populated directly by helicity-flip scattering if the neutrino mass is large enough, and this property has been used to infer a bound of $m_{\nu_\tau} \lesssim 1$ MeV taking $N_\nu < 4$ [76]. If there is mixing between active and sterile neutrinos then the effect on BBN is more complicated [77].

The limit on the expansion rate during BBN can also be translated into bounds on the mass/lifetime of non-relativistic particles which decay during BBN. This results in an even faster speed-up rate, and typically also change the entropy [78]. If the decays include Standard Model particles, the resulting electromagnetic [79–80] and/or hadronic [81] cascades can strongly perturb the light elements, which leads to even stronger constraints. Such arguments have been applied to rule out a MeV mass ν_τ, which decays during nucleosynthesis [82].

Such arguments have proved very effective in constraining supersymmetry. For example, if the gravitino is very light and contributes to g_*, the illustrative BBN limit $N_\nu < 4$ requires its mass to exceed ~ 1 eV [83]. Alternatively, much recent interest has focussed on the case in which the next-to-lightest supersymmetric particle is metastable and decays during or after BBN. The constraints on unstable particles discussed above imply stringent bounds on the allowed abundance of such particles [81]; if the metastable particle is charged (*e.g.*, the stau), then it is possible for it to form atom-like electromagnetic bound states with nuclei, and the resulting impact on light elements can be quite complex [84]. Such decays can destroy ^{7}Li and/or produce ^{6}Li, leading to a possible supersymmetric solution to the lithium problems noted above [85](see [4] for a review). In addition, these arguments impose powerful constraints on supersymmetric inflationary cosmology [80–81], in particular thermal leptogenesis [86]. These can be evaded only if the gravitino is massive enough to decay before BBN, *i.e.*, $m_{3/2} \gtrsim 50$ TeV [87](which would be unnatural), or if it is in fact the lightest supersymmetric particle and thus stable [80,88]. Similar constraints apply to moduli – very weakly coupled fields in string theory which obtain an electroweak-scale mass from

supersymmetry breaking [89].

Finally, we mention that BBN places powerful constraints on the possibility that there are new large dimensions in nature, perhaps enabling the scale of quantum gravity to be as low as the electroweak scale [90]. Thus, Standard Model fields may be localized on a 'brane,' while gravity alone propagates in the 'bulk.' It has been further noted that the new dimensions may be non-compact, even infinite [91], and the cosmology of such models has attracted considerable attention. The expansion rate in the early Universe can be significantly modified, so BBN is able to set interesting constraints on such possibilities [92].

References:

1. R.V. Wagoner *et al.*, Astrophys. J. **148**, 3 (1967).
2. R.A. Malaney & G.J. Mathews, Phys. Reports **229**, 145 (1993).
3. S. Sarkar, Rept. on Prog. in Phys. **59**, 1493 (1996).
4. K. Jedamzik & M. Pospelov, New J. Phys. **11**, 105028 (2009).
5. D.N. Schramm & M.S. Turner, Rev. Mod. Phys. **70**, 303 (1998).
6. K.A. Olive *et al.*, Phys. Reports **333**, 389 (2000).
7. P.J.E. Peebles, Phys. Rev. Lett. **16**, 411 (1966).
8. J. Bernstein *et al.*, Rev. Mod. Phys. **61**, 25 (1989).
9. S. Mukhanov, Int. J. Theor. Phys. **143**, 669 (2004).
10. R. Esmailzadeh *et al.*, Astrophys. J. **378**, 504 (1991).
11. R.H. Cyburt *et al.*, JCAP **0811**, 012 (2008).
12. R.H. Cyburt *et al.*, New Astron. **6**, 215 (2001).
13. L. Kawano, FERMILAB-PUB-92/04-A.
14. O. Pisanti *et al.*, Comput. Phys. Commun. **178**, 956 (2008).
15. S. Esposito *et al.*, Nucl. Phys. **B568**, 421 (2000).
16. S. Dodelson & M.S. Turner, Phys. Rev. **D46**, 3372 (1992).
17. D. Seckel, `hep-ph/9305311`;
    R. Lopez & M.S. Turner, Phys. Rev. **D59**, 103502 (1999).
18. M.S. Smith *et al.*, Astrophys. J. Supp. **85**, 219 (1993).
19. G. Fiorentini *et al.*, Phys. Rev. **D58**, 063506 (1998).
20. K.M. Nollett & S. Burles, Phys. Rev. **D61**, 123505 (2000).
21. A. Coc *et al.*, Astrophys. J. **600**, 544 (2004).
22. R.H. Cyburt, Phys. Rev. **D70**, 023505 (2004).
23. P.D. Serpico *et al.*, JCAP **12**, 010 (2004).
24. R.H. Cyburt & B. Davids, Phys. Rev. **C78**, 012 (2008).
25. K.M. Nollett *et al.*, Astrophys. J. Lett. **552**, L1 (2001).
26. S. D'Odorico *et al.*, Astron. & Astrophys. **368**, L21 (2001).
27. M. Pettini & D. Bowen, Astrophys. J. **560**, 41 (2001).
28. J.M. O'Meara *et al.*, Astrophys. J. Lett. **649**, L61 (2006).
29. M. Pettini *et al.*, MNRAS **391**, 1499 (2008).
30. R.I. Epstein *et al.*, Nature **263**, 198 (1976).
31. B.E. Wood *et al.*, Astrophys. J. **609**, 838 (2004).
32. J.L. Linsky *et al.*, Astrophys. J. **647**, 1106 (2006).

33. B.D. Savage *et al.*, Astrophys. J. **659**, 1222 (2007).
34. B.D. Fields, Astrophys. J. **456**, 678 (1996).
35. D. Kirkman *et al.*, Astrophys. J. **529**, 655 (2000).
36. Y.I. Izotov *et al.*, Astrophys. J. **527**, 757 (1999).
37. K.A. Olive & E. Skillman, Astrophys. J. **617**, 29 (2004).
38. Y.I. Izotov *et al.*, Astrophys. J. **662**, 15 (2007).
39. M. Peimbert *et al.*, Astrophys. J. **667**, 636 (2007).
40. N. Christlieb *et al.*, Nature **419**, 904 (2002).
41. M. Spite & F. Spite, Nature **297**, 483 (1982).
42. S.G. Ryan *et al.*, Astrophys. J. **523**, 654 (1999).
43. E. Vangioni-Flam *et al.*, New Astron. **4**, 245 (1999).
44. S.G. Ryan *et al.*, Astrophys. J. Lett. **530**, L57 (2000).
45. P. Bonifacio *et al.*, Astron. & Astrophys. **390**, 91 (2002).
46. J. Meléndez & I. Ramirez, Astrophys. J. Lett. **615**, 33 (2004).
47. P. Bonifacio *et al.*, Astron. & Astrophys. **462**, 851 (2007).
48. M.H. Pinsonneault *et al.*, Astrophys. J. **574**, 389 (2002).
49. A.J. Korn *et al.*, Nature **442**, 657 (2006).
50. M. Asplund *et al.*, Astrophys. J. **644**, 229 (2006).
51. R. Cayrel *et al.*, Astron. & Astrophys. **473**, L37 (2007).
52. T.M. Bania *et al.*, Nature **415**, 54 (2002).
53. K.A. Olive *et al.*, Astrophys. J. **479**, 752 (1997).
54. E. Vangioni-Flam *et al.*, Astrophys. J. **585**, 611 (2003).
55. H. Reeves *et al.*, Astrophys. J. **179**, 909 (1973).
56. M. Fukugita & P.J.E. Peebles, Astrophys. J. **616**, 643 (2004).
57. R. Cen & J.P. Ostriker, Astrophys. J. **514**, 1 (1999).
58. G. Jungman *et al.*, Phys. Rev. **D54**, 1332 (1996).
59. M. Tegmark *et al.*, Phys. Rev. **D63**, 043007 (2001).
60. J. Dunkley *et al.*, Astrophys. J. Supp. **180**, 306 (2009).
61. P. Hunt & S. Sarkar, Phys. Rev. **D76**, 123504 (2007).
62. K. Jedamzik & J.B. Rehm, Phys. Rev. **D64**, 023510 (2001).
63. D.J. Fixsen *et al.*, Astrophys. J. **473**, 576 (1996).
64. R.H. Cyburt *et al.*, Phys. Lett. **B567**, 227 (2003).
65. G. Steigman *et al.*, Phys. Lett. **B66**, 202 (1977).
66. R.H. Cyburt *et al.*, Astropart. Phys. **23**, 313 (2005).
67. E. Lisi *et al.*, Phys. Rev. **D59**, 123520 (1999).
68. V. Barger *et al.*, Phys. Lett. **B566**, 8 (2003).
69. E.W. Kolb *et al.*, Phys. Rev. **D33**, 869 (1986);
    F.S. Accetta *et al.*, Phys. Lett. **B248**, 146 (1990);
    B.A. Campbell & K.A. Olive, Phys. Lett. **B345**, 429 (1995);
    K.M. Nollett & R. Lopez, Phys. Rev. **D66**, 063507 (2002);
    C. Bambi *et al.*, Phys. Rev. **D71**, 123524 (2005).
70. A. Coc *et al.*, Phys. Rev. **D73**, 083525 (2006).
71. K.A. Olive *et al.*, Nucl. Phys. **B180**, 497 (1981).
72. J. Ellis *et al.*, Phys. Lett. **B167**, 457 (1986).

73. L.M. Krauss *et al.*, Phys. Rev. Lett. **71**, 823 (1993).
74. J.A. Morgan, Phys. Lett. **B102**, 247 (1981).
75. E.W. Kolb *et al.*, Phys. Rev. **D34**, 2197 (1986);
J.A. Grifols & E. Massó, Mod. Phys. Lett. **A2**, 205 (1987);
K.S. Babu *et al.*, Phys. Rev. Lett. **67**, 545 (1991).
76. A.D. Dolgov *et al.*, Nucl. Phys. **B524**, 621 (1998).
77. K. Enqvist *et al.*, Nucl. Phys. **B373**, 498 (1992);
A.D. Dolgov, Phys. Reports **370**, 333 (2002).
78. K. Sato & M. Kobayashi, Prog. Theor. Phys. **58**, 1775 (1977);
D.A. Dicus *et al.*, Phys. Rev. **D17**, 1529 (1978);
R.J. Scherrer & M.S. Turner, Astrophys. J. **331**, 19 (1988).
79. D. Lindley, MNRAS **188**, 15 (1979), Astrophys. J. **294**, 1 (1985).
80. J. Ellis *et al.*, Nucl. Phys. **B259**, 175 (1985);
J. Ellis *et al.*, Nucl. Phys. **B373**, 399 (1992);
R.H. Cyburt *et al.*, Phys. Rev. **D67**, 103521 (2003).
81. M.H. Reno & D. Seckel, Phys. Rev. **D37**, 3441 (1988);
S. Dimopoulos *et al.*, Nucl. Phys. **B311**, 699 (1989);
K. Kohri *et al.*, Phys. Rev. **D71**, 083502 (2005).
82. S. Sarkar & A.M. Cooper, Phys. Lett. **B148**, 347 (1984).
83. J.A. Grifols *et al.*, Phys. Lett. **B400**, 124 (1997).
84. M. Pospelov *et al.*, Phys. Rev. Lett. **98**, 231301 (2007);
R.H. Cyburt *et al.*, JCAP **11**, 014 (2006);
M. Kawasaki *et al.*, Phys. Lett. **B649**, 436 (2007).
85. K. Jedamzik *et al.*, JCAP **07**, 007 (2006).
86. S. Davidson *et al.*, Phys. Rev. **466**, 105 (2008).
87. S. Weinberg, Phys. Rev. Lett. **48**, 1303 (1979).
88. M. Bolz *et al.*, Nucl. Phys. **B606**, 518 (2001).
89. G. Coughlan *et al.*, Phys. Lett. **B131**, 59 (1983).
90. N. Arkani-Hamed *et al.*, Phys. Rev. **D59**, 086004 (1999).
91. L. Randall & R. Sundrum, Phys. Rev. Lett. **83**, 3370 (1999).
92. J.M. Cline *et al.*, Phys. Rev. Lett. **83**, 4245 (1999);
P. Binetruy *et al.*, Phys. Lett. **B477**, 285 (2000).